

Synthesis and Characterization of Tetrafunctional Lactic Acid Oligomers: A Potential *In Situ* Forming Degradable Orthopaedic Biomaterial

JASON A. BURDICK,¹ LANEY M. PHILPOTT,¹ KRISTI S. ANSETH^{1,2}

¹ Department of Chemical Engineering, University of Colorado, ECCH 111, Boulder, Colorado 80309-0424

² Howard Hughes Medical Institute, University of Colorado, ECCH 111, Boulder, Colorado 80309-0424

Received 13 November 2000; accepted 20 December 2000

ABSTRACT: Tetrafunctional lactic acid oligomers with low molecular weight ethylene glycol cores were synthesized and characterized to assess their applicability to orthopaedics. Utilizing a visible light photoinitiating system, these oligomers polymerize within minutes to form highly crosslinked networks and, thus, have potential for *in situ* formation. Varying the oligomer structure readily alters the physical properties of the resultant polymer networks. For instance, mechanical properties were highly dependent on the number of lactic acid and ethylene glycol units in the oligomer backbone. Additionally, polymer mass loss ranged from ~30 to 60% within 8 weeks of degradation time depending on the oligomer chemistry. Mechanical properties decreased with degradation of these polymers, indicating a bulk degradation mechanism. Finally, scaffolds with a controlled architecture were fabricated from these oligomers that show potential for tissue-engineering applications. © 2001 John Wiley & Sons, Inc. *J Polym Sci A: Polym Chem* 39: 683–692, 2001

Keywords: photopolymerization; poly(lactic acid); orthopaedic biomaterials; bone-tissue engineering

INTRODUCTION

Degradable polymers are being investigated for a wide range of orthopaedic applications, including scaffolds for bone-tissue engineering,¹ delivery of biologically active drugs for enhanced bone growth,² and degradable implants for fracture fixation.³ The benefits of degradable polymers for orthopaedic applications are many and include the ability to achieve a wide range of properties related to mechanics, degradation, and biological response.^{4,5} Also, a second surgery is not necessary for implant removal when a degradable polymer is used in place of metal implants or hardware.

One specific orthopaedic application that can benefit from recent advances in synthetic degradable polymers is an alternative for bone auto- and allografts. Typical treatments for large bone defects, resulting from severe patient trauma or tumor removal, include bone grafting with autograft and/or allograft materials. Autografts suffer from limited donor sites as well as the occurrence of tissue morbidity at the donor site.⁶ Allografts are limited by the compatibility between the donor and the patient and vascular integration.⁷ Failure rates for grafted materials have been reported as high as 50%.⁸ Therefore, a synthetic replacement for bone grafts would be very beneficial; however, potential polymeric graft replacements need to have a controllable degradation mechanism, be readily fabricated into scaffolds with a potentially complex macroscopic architecture, facilitate adhesion of cells necessary

Correspondence to: K. S. Anseth (E-mail: kristi.anseth@colorado.edu)

Journal of Polymer Science: Part A: Polymer Chemistry, Vol. 39, 683–692 (2001)
© 2001 John Wiley & Sons, Inc.

for extracellular matrix deposition, and maintain a sufficient three-dimensional structure long enough for tissue formation.

Numerous researchers have investigated degradable polyesters such as poly(lactic acid) (PLA), poly(glycolic acid) (PGA), and their copolymers (PLGA) for medical applications, including orthopaedics.⁵ These polymers, widely used as degradable sutures, have a long-standing history in medical applications, supporting their biocompatibility. In these materials, degradation occurs throughout the bulk of the polymer resulting in a nonlinear mass loss, a decrease in mechanical properties with time, and a burst of acidic degradation products toward the end of degradation. Several researchers have shown that osteoblasts readily attach, migrate, and proliferate on these polyesters, and many studies indicate that PLA, PGA, and PLGA have good potential for bone-tissue-engineering applications.^{9,10}

In contrast to linear, degradable polyesters, our group has recently developed multifunctional anhydride monomers that react to form highly crosslinked networks via a photoinitiated polymerization.¹¹ Because the photopolymerization conditions are sufficiently mild, these monomers can be reacted *in situ* in the body. *In situ* forming materials can eliminate some of the problems associated with fabricating scaffolds outside of the body into complex shapes that fit bone defects. The degradation rate of the final polymer networks is controlled by the hydrophobicity of the monomers, and degradation times of a couple of days up to a year¹² can be achieved by copolymerizing various monomers. The networks surface erode, which allow for a controlled and sustained release of encapsulated molecules for drug-delivery applications. Additionally, in contrast to bulk-degrading PLA and PGA, these polymers maintain mechanical integrity with degradation,³ which may provide additional benefits in load-bearing orthopaedic applications. Despite these benefits, the polyanhydride degradation mechanism limits cell attachment and proliferation. The surface of these networks is continually eroded with time, which hinders the attachment of anchorage-dependent osteoblasts.

Hubbell and coworkers¹³ have synthesized *in situ* forming hydrogels from water-soluble, photocrosslinkable poly(ethylene glycol)(PEG)-co-poly(α -hydroxy acid) macromers with applications ranging from drug delivery to adhesion prevention.¹⁴ Additionally, this group has studied macromers with a higher functionality and lower molecular weights to produce more densely

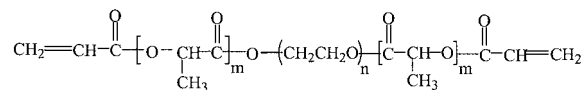


Figure 1. Chemical structure of multifunctional lactic acid oligomer with oligo(ethylene glycol) core.

crosslinked networks.¹⁵ Specific applications of these highly crosslinked networks include polymer scaffolds with cell repellency that can be subsequently modified with bioactive factors for selective cell adhesion. Using similar macromer chemistry, Kim and coworkers¹⁶ investigated applications for these materials as biodegradable lubricants for coating medical products.

The present work encompasses the development and characterization of reactive multifunctional oligomers based on similar chemistries used by Sawhney et al.¹³ to produce degradable hydrogels that could potentially serve as a synthetic bone-graft replacement. Specifically, low molecular weight oligo(lactic acid) molecules end capped with acrylate groups were synthesized. In the present article, the degradation mechanism and mechanical properties of the resulting polymer networks were studied as a function of the oligomer chemistry. Additionally, the ability to form scaffolds with controlled macroscopic architecture with the potential to serve as a replacement for bone grafts is presented.

EXPERIMENTAL

Oligomer Synthesis

Tetrafunctional lactic acid oligomers (Fig. 1) were synthesized by a ring-opening polymerization of lactide on low molecular weight ethylene glycol cores that were subsequently acrylated in a manner similar to previous work by Hubbell and coworkers.¹³ Briefly, oligomers of ethylene glycol were reacted with *d,l*-lactide for 6 h at 150 °C under vacuum. Stannous octoate (1 : 200 molar ratio to *d,l*-lactide) was added dropwise for reaction catalysis. After cooling to room temperature, the product was dissolved in methylene chloride, and a 1.1 molar ratio of triethylamine was added. A 1.1 molar ratio of acryloyl chloride in a methylene chloride solution (1 : 10 volume ratio) was added dropwise over several hours at 0 °C. This reaction was left at room temperature for approximately 36 h; triethylamine hydrochloride was filtered from the solution; and, finally, the product was precipitated in hexane. All chemicals were

obtained from Aldrich and used as received, except *d,l*-lactide was obtained from Polysciences.

Specific oligomers investigated in this study consisted of diethylene glycol with ~ 6 lactides on each side (2EG6LA), diethylene glycol with ~ 10 lactides on each side (2EG10LA), and PEG-400 with ~ 6 lactides on each side (8EG6LA). These oligomers were functionalized by acrylating both ends of the molecule. These oligomers were chosen and characterized to determine the effect of alterations in the oligomer chemistry on macroscopic properties such as mechanics, degradation, and mass loss. The chemical structures of the oligomers were characterized with NMR (Varian Unity Inova-500) to quantify the length of the lactide blocks and the acrylation efficiency.

Polymerization Characterization

A visible-light-initiating system of equal masses of camphorquinone (widely used in the dental field) and ethyl-4-*N,N*-dimethylaminobenzoate (CQ/4EDMAB) was used for all polymerizations. This specific initiator system is known to be relatively cytocompatible when polymerized directly in the presence of cells.¹⁷ Initiation conditions included initiator concentrations of 1.0 and 0.5 wt % and visible-light (400–500 nm) intensities of 50 and 25 mW/cm² from an EFOS Novacure light source. These parameters were chosen to determine the effects of initiation conditions on the time for polymerization and double-bond conversion. Polymerization rates were monitored as a function of polymerization time at room temperature as well as in the presence of oxygen with DSC (Perkin–Elmer, DSC7). Isothermal conditions were maintained with an external chiller (NESLAB RTE-111) attached to the DSC. For analysis, 2–3 mg of oligomer with initiator were placed uniformly on the bottom of an aluminum DSC pan, and the heat flux, which is directly proportional to the rate of polymerization, was monitored during irradiation for ~ 10 min.

Fourier transform infrared spectroscopy (FTIR) (Nicolet Magna-IR 750 Series II) was used to monitor the double-bond conversion with time.¹⁸ The monomer–initiator composition was sandwiched between two salt crystals and placed in a horizontal sample holder. The same initiation conditions used in the DSC studies were followed. The area of the acrylate peak (~ 1637 cm⁻¹) was measured in real time while irradiating the sample with visible light and used to calculate the double-bond conversion. Reaction characterization studies were performed in duplicate.

Polymer Physical and Mechanical Properties

Oligomers were polymerized with 0.5 wt % initiator (CQ/EDMAB) and ~ 25 mW/cm² visible light (450 nm, Electro-Lite Corporation) for 30 min to ensure complete conversion. The liquid oligomer–initiator solutions were placed in Teflon molds between glass slides and photopolymerized. The relative hydrophobicity of the polymers was characterized by measuring the contact angle of water on the polymer surface. This measurement was repeated on both surfaces of five polymer samples for each composition. The sol fraction was determined by swelling a polymer disk (5-mm diameter, 1-mm thick) in methylene chloride for 24 h, removing the polymer, drying in a vacuum oven, and measuring the dry mass of at least three polymers for each composition.

A dynamic mechanical analyzer (Perkin–Elmer, DMA7) operated in extension mode was used to characterize the viscoelastic nature of these polymers. Rectangular polymer slabs, approximately 10 mm long, 5 mm wide, and 1 mm depth, were mounted with a sinusoidal force of ~ 3000 mN while ramping the temperature from -60 to 60 °C at a rate of 5 °C/min. The storage and loss modulus were recorded as a function of increasing temperature. To prevent the sample from breaking, dynamic control was implemented after the loss-tangent curve reached a maximum. The glass-transition temperature was reported from the peak of the loss-tangent curve. This analysis was repeated in triplicate for each oligomer studied.

Tensile strengths of the polymerized samples were determined using an SMS Material Tester (Micro MT100, MonoResearch, NY). I-beam shaped samples were prepared according to ASTM standard D695-91 with a gauge length of 20 mm, width of 5 mm, and thickness of 1 mm. Samples were strained at a rate of 0.1 mm/s until macroscopic failure occurred. The tensile modulus was calculated from the slope of the resulting stress-versus-strain curve. The ultimate tensile strength and the strain at break were also recorded.

Polymer Degradation

Polymer disks with a diameter of 5 mm and a thickness of 1 mm were degraded in phosphate buffered saline (PBS) at 37 °C on an orbital shaker. The PBS solution was changed every 2–3 d, and samples (three per oligomer composition for each timepoint) were removed every week for

analysis. The compressive modulus of the samples was determined using a Perkin–Elmer DMA Parallel Plate Measuring System to monitor changes in mechanical properties with degradation. Polymer disks were placed between parallel plates at room temperature, and the applied force was ramped from 5.0 to 5000.0 mN at a rate of 200.0 mN/min. The compressive modulus was calculated using the slope of the linear region of the stress-versus-strain curve when less than 10% deformation had occurred. These same samples were subsequently dried in a vacuum oven for 24 h. The percent mass loss was calculated from the difference in the original mass before degradation and the dried mass after degradation divided by the initial mass.

Scaffold Fabrication and Characterization

Porous scaffolds were formed using a particulate leaching technique previously developed by Mikos et al.¹⁹ The oligomer and initiator were dissolved in methylene chloride and physically mixed with sodium chloride crystals that were previously ground and sieved according to their size. This approach allowed for thorough mixing of the oligomer and poragen. The methylene chloride was allowed to evaporate, and the mixture was placed in Teflon molds and polymerized with ~25 mW/cm² visible light for 30 min. The sodium chloride was leached from the scaffold in several changes of deionized water over 24 h.

Scaffolds with various pore sizes and ratios of oligomer to poragen were fabricated and viewed using scanning electron microscopy (SEM) (ISI SX30). After drying of the scaffolds, the samples were frozen in liquid nitrogen and fractured. Scaffold cross sections were sputter-coated with gold and viewed with SEM. The scaffold architecture was followed as a function of degradation for up to 6 weeks.

RESULTS AND DISCUSSION

Oligomer Synthesis

Oligomers that form highly crosslinked and degradable networks via a photoinitiated polymerization were synthesized. These oligomers were rationally designed to meet properties that are desired for a biomaterial that could potentially replace current bone-graft materials. The effect of oligomer chemistry on the resulting polymer network's mechanical properties, degradation be-

Table I. Oligomer Properties As Characterized Using NMR

Oligomer	% Acrylation	Number of Lactides per Side	Molecular Weight (g/mol)
2EG6LA	96.0	6.3	990
2EG10LA	92.3	10.0	1450
8EG6LA	90.7	5.9	1240

havior, and mass loss was investigated. Specifically, oligomers with variations in the core molecule or number of ethylene glycol repeat units and variations in the number of lactic acid repeat units were studied.

Table I outlines the oligomers that were studied along with NMR characterization of the length of the PLA blocks and the percent acrylation. The length of PLA blocks is important when discussing polymer properties such as degradation and mechanics (crosslinking density). Additionally, the percent acrylation affects network-gelation properties as well as mechanics.

Polymerization Characterization

The rate of polymerization was monitored during the photoinitiated polymerization of 2EG10LA, which exhibits typical behavior observed in all of the oligomers studied. The rate profile as a function of time is shown in Figure 2 for a variety of initiation conditions. The shape of the rate profile is indicative of the many complexities that occur during the polymerization of multifunctional monomers. At short times, the polymerization rate increases dramatically during a period of autoacceleration when termination is diffusion controlled. As the rate of polymerization approaches its maximum, propagation becomes diffusion controlled, and the polymerization rate autodecelerates. Under relatively mild initiation conditions the polymerization is essentially complete within a couple of minutes.

These results indicate that the rate of polymerization is highly dependent on the initiation conditions. For example, the maximum rate is reached with the highest initiator concentration and highest light intensity (i.e., 1.0 wt % photoinitiator and 50 mW/cm² visible light), and, likewise, the lowest initiator concentration and lowest light intensity (i.e., 0.5 wt % photoinitiator and 25 mW/cm²) led to the lowest rates of polymerization. Both the initiator concentration and

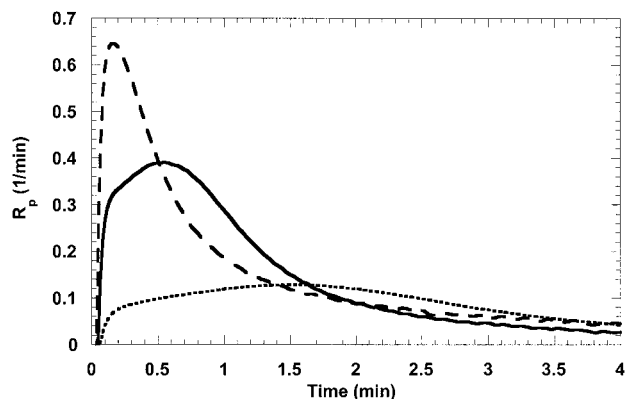


Figure 2. Rate of polymerization versus time for initiation of 2EG10LA with various initiator concentrations and light intensities: 1.0 wt % CQ/4EDMAB and 50 mW/cm² visible light (dashed line), 0.5 wt % CQ/4EDMAB and 50 mW/cm² visible light (solid line), and 0.5 wt % CQ/4EDMAB and 25 mW/cm² visible light (dotted line).

the light intensity were changed independently to determine that each parameter has an effect on the polymerization rates. In general, the polymerization rate did not scale with the rate of initiation to the half-power, but rather with the rate of initiation to the 0.7 power. During multifunctional acrylate polymerizations, others have observed a dependence ranging from 0.5 to 1.0.²⁰

The double-bond conversion under these same conditions was monitored using FTIR, and the double-bond conversion as a function of time is shown in Figure 3. Again, the initiation conditions (i.e., initiator concentration and light intensity) were altered in these studies. These results indicate that the initiation conditions affect both the maximum attainable double-bond conversion of the network and the time that is necessary to reach that conversion. For example, ~80% conversion is reached within 2 min in a system that is initiated with 1.0 wt % photoinitiator and 50 mW/cm² visible light, but less than 60% conversion is reached in 10 min in a system initiated with 0.5 wt % photoinitiator and 25 mW/cm² visible light. From the combined FTIR and DSC data, the heat evolved per acrylate double bond was calculated to be ~17.5 kcal/mol, which is within the range of previous results for acrylate polymerizations.²¹

Because 2EG10LA is still in a transition period from a glassy to a rubbery network at room temperature, complete conversion is not expected. Mobility of reacting species is more limited in glassy polymers than in rubbery networks, and,

thus, the achievement of high conversions is difficult. Additionally, differences in double-bond conversions may be attributed to temperature rises during the exothermic photopolymerization. As shown previously,²² initiation conditions dramatically affect properties such as the exothermic temperature rise for polymerization of vinyl monomers. Differences in the ultimate double-bond conversions may also be directly related to the rate of initiation and the subsequent differences in network volume relaxation. In systems polymerized quickly, the rate of volume relaxation is much slower than the rate of polymerization, which can lead to excess free volume and, ultimately, higher double-bond conversions in systems that are polymerized at a faster rate.²³ From an application viewpoint, it should be noted that the light intensities studied are relatively low, and higher conversions are expected when a higher visible-light intensity or a more efficient initiator (e.g., those used with ultraviolet light) is used for initiation. The extractable sol fraction relates to the double-bond conversion; therefore, maximizing the double-bond conversion is important to reduce potential toxicity from unreacted oligomer.

The results of these reaction-characterization studies illustrate that the oligomer studied forms a highly crosslinked network with relatively high conversion (0.60–0.85) in very short time periods (2–10 min) with low visible-light intensities (25–50 mW/cm²). For an *in situ* forming orthopaedic biomaterial, high conversions are desirable in the span of several minutes for ease of application

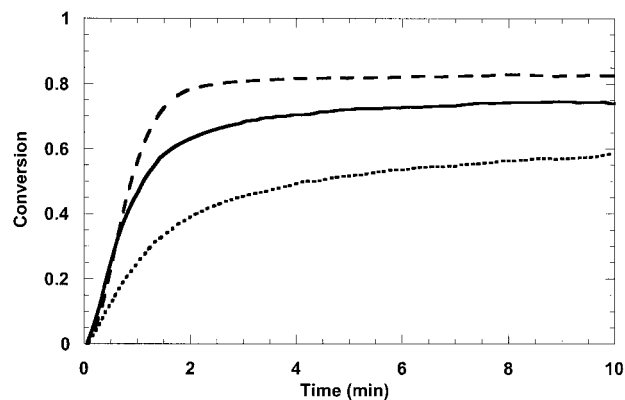


Figure 3. Conversion versus time for initiation of 2EG10LA with various initiator concentrations and light intensities: 1.0 wt % CQ/4EDMAB and 50 mW/cm² visible light (dashed line), 0.5 wt % CQ/4EDMAB and 50 mW/cm² visible light (solid line), and 0.5 wt % CQ/4EDMAB and 25 mW/cm² visible light (dotted line).

Table II. Physical Properties of Polymer Networks

Oligomer	Sol Fraction ^a	Contact Angle (°)	T_g (°C)
2EG6LA	11.0 ± 3.0	133.0 ± 8.0	26.7 ± 0.2
2EG10LA	2.3 ± 1.0	123.6 ± 7.3	22.0 ± 0.7
8EG6LA	3.1 ± 1.9	142.0 ± 5.2	1.8 ± 0.2

^a Polymerized with 0.5 wt % CQ/EDMAB and ~25 mW/cm² visible light for 30 min.

in the operating room. Additionally, these studies show that the rate of polymerization may be tailored for specific applications depending on the initiation conditions. Although high rates of polymerization are desirable for most orthopaedic applications, lower rates may be necessary for applications such as protein delivery where a high rate of initiation can lead to significant temperature excursions.²²

Polymer Physical and Mechanical Properties

Several physical properties of the polymer networks were studied, and the results are summarized in Table II. The sol fraction was highest for the 2EG6LA oligomer, attributed to its lower molecular weight that produces a densely crosslinked network when polymerized at room temperature. The higher crosslinking density and higher glass-transition temperature, when compared to other oligomers studied, leads to low mobility of the reacting species in the network and a maximum double-bond conversion that is less than one. This issue is especially prevalent when comparing polymers with significantly different glass-transition temperatures.

The relative hydrophobicity of these polymers was characterized by water-contact-angle measurements on polymer films. The results indicate that the hydrophobicity of the polymers was highly dependent on the oligomer chemistry. The 2EG10LA oligomer with a contact angle of ~124° was found to be significantly more hydrophobic than 8EG6LA with a contact angle of ~142°. The 2EG10LA oligomer is comprised mainly of hydrophobic PLA, whereas 8EG6LA has a higher proportion of hydrophilic ethylene glycol repeat units. The polymer hydrophobicity is important when analyzing properties such as polymer degradation and cell attachment. Specifically, more hydrophobic polymers facilitate protein adsorption, which can result in a more readily attachment of cells.²⁴ Additionally, these polymers ex-

hibited no measurable swelling in PBS at short times because of the combined hydrophobicity and high crosslinking density of the polymer networks.

The viscoelastic properties of the polymer networks were determined as a function of network composition and crosslinking density by measuring the storage modulus as a function of temperature using a DMA. Polymerization of multifunctional monomers is nonideal and can lead to numerous structural heterogeneities in the network (e.g., distribution of crosslinks, trapped radicals, and unreacted oligomer).²⁵ These heterogeneities can lead to a broad distribution of mobility in the network as well as a broad T_g .

The storage modulus as a function of temperature is shown in Figure 4(a) for polymer networks formed from 2EG10LA and 8EG6LA. The storage modulus of these polymers is similar at low temperatures when the polymers are in the glassy regime. The magnitude of the storage modulus (~1 GPa) at these low temperatures is indicative of a highly crosslinked, glassy network. As the

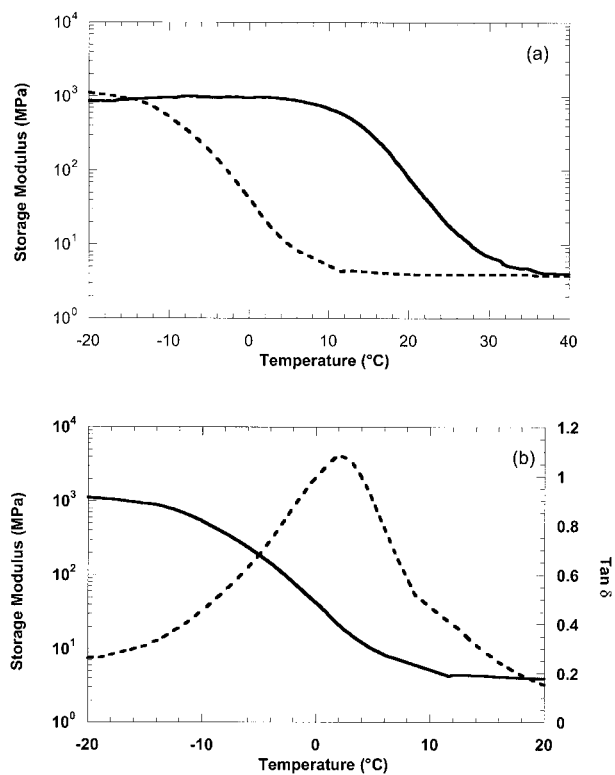


Figure 4. Viscoelastic behavior of polymers with temperature variation: (a) storage modulus versus temperature for poly(2EG10LA) (solid line) and poly(8EG6LA) (dashed line) and (b) storage modulus (solid line) and $\text{Tan } \delta$ (dashed line) versus temperature of poly(8EG6LA).

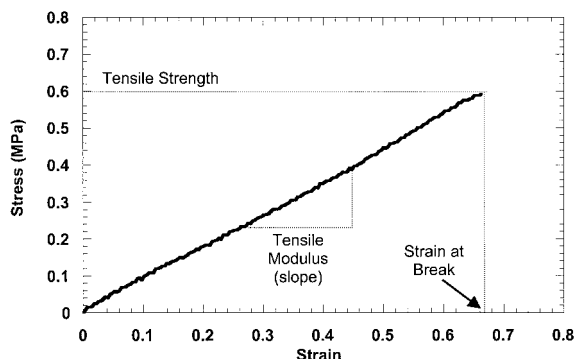


Figure 5. Stress-versus-strain data for tensile testing of poly(2EG6LA) (the shape of this plot is representative of all oligomers tested).

temperature is increased, the more hydrophilic poly(8EG6LA) network exhibits a T_g region from ~ -20 to 10 °C, compared to poly(2EG10LA) where a T_g region is present from ~ 10 to 35 °C. The heterogeneity of these networks produces a transition region that spans over ~ 30 °C. Both of these polymers are in their rubbery region at physiological temperatures (~ 37 °C). Interestingly, for the two networks shown, although the molecular weight of the original oligomers 2EG10LA and 8EG6LA is significantly different, the final crosslinking densities in the polymer network are similar (as indicated by the magnitude of the storage modulus in the rubbery plateau). This observation indicates the importance of factors such as cyclization and crosslinking, in addition to overall oligomer structure, on the macroscopic mechanical properties.

To more clearly illustrate the T_g region, the loss tangent is plotted as a function of temperature in Figure 4(b) for the poly(8EG6LA) network. The peak in the $\tan \delta$ curve occurs at the inflection point of the storage-modulus curve and is used to identify the T_g values listed in Table II. As reported in Table II, the T_g value is ~ 25 °C different between the networks synthesized from the 2EG6LA and 8EG6LA oligomers. This variance may be attributed to both the differences in chemistry and crosslinking density between the networks.

To further understand the mechanical properties of these polymer networks and their dependence on the initial oligomer structure, the tensile properties of the polymers were measured using a static material tester. A representative data set from these tests is shown in Figure 5 for poly(2EG6LA). In general, the stress-versus-strain curves were linear until sample failure.

The tensile modulus, tensile strength, and strain at break for the polymers are summarized in Table III.

For a given temperature above the sample's T_g value, the tensile modulus is proportional to the number of effective crosslinks and therefore related to the crosslinking of the polymer network. For example, the polymer formed from 2EG6LA had a tensile modulus almost four times higher than that from 2EG10LA. Although the chemistry of these oligomers is similar, the molecular weight is different because of the increased number of lactide units on 2EG10LA. Both the strain at break and the tensile strength are dependent on the oligomer chemistry. For instance, the strain at break was highest for 2EG10LA and lowest for 8EG6LA. Because the strain is correlated to the elongation that is possible for each sample, these results show that the chemistry has a dramatic effect on the mechanics and, in this case, rubbery nature of the sample. From previous results, although the 8EG6LA is in a rubbery regime at room temperature, whereas 2EG10LA is still in a transition period, the polymer from 2EG10LA elongates much more before breaking. Additionally, the tensile strength is much higher for 2EG6LA than for 8EG6LA. Although there is some dependence on crosslinking density, because 2EG10LA is almost three times higher than 8EG6LA, there is also a dependence on the oligomer chemistry.

Polymer Degradation

An understanding of both the degradation time and the degradation mechanism is necessary for the intended orthopaedic applications. As seen in Figure 6, these polymers have a complex mass-loss profile that is strongly coupled to the network structure and chemistry. A decrease of $\sim 10\%$ in mass is seen within the first week, which was mainly attributed to release of the sol fraction and oxygen inhibition effects at the polymer surfaces during polymerization (i.e., unreacted oli-

Table III. Polymer Mechanical Properties

Oligomer	Tensile Modulus (MPa)	Strain at Break	Tensile Strength (MPa)
2EG6LA	3.67 ± 0.28	0.47 ± 0.02	1.74 ± 0.18
2EG10LA	0.92 ± 0.05	0.65 ± 0.02	0.63 ± 0.03
8EG6LA	1.27 ± 0.19	0.19 ± 0.03	0.23 ± 0.02

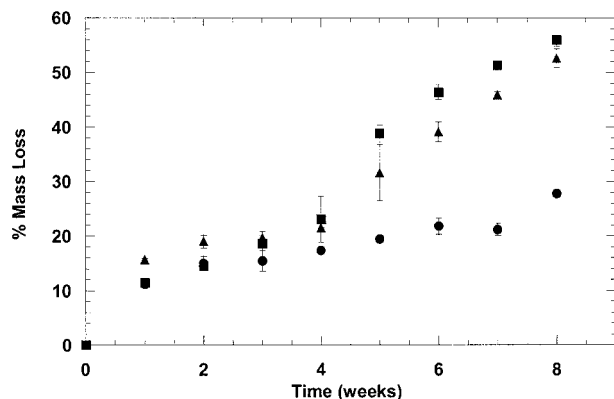


Figure 6. Mass loss of polymer disks with degradation in PBS at 37 °C: (▲) poly(2EG6LA); (●) poly(2EG10LA); (■) poly(8EG6LA).

gomer at the surface). After 1 week, the mass loss remains relatively linear for up to 1 month of degradation, and then significant differences between the networks are observed. For the hydrophilic poly(8EG6LA), some swelling was observed around 4 weeks, plasticizing the network and allowing degradation products to more readily diffuse from the crosslinked polymer. Although no swelling was observed for poly(2EG6LA), a similar trend is seen. The slightly slower degradation rate was attributed to both the crosslinking density and hydrophobicity of the polymers. Interestingly, for poly(2EG10LA) the degradation was the slowest with only ~30% mass loss after 8 weeks of degradation compared to almost 60% mass loss for poly(8EG6LA). Although this polymer has the most lactide units in each crosslink, making the probability of hydrolysis of each crosslink higher, the hydrophobicity of poly(2EG10LA) makes it difficult for water to penetrate the network. Thus, mechanical property measurements with degradation can provide additional insight related to the cleavage of crosslinks with time as compared to the mass loss with time.

For numerous orthopaedic applications of polymeric biomaterials, the mechanics with degradation are especially important. Therefore, the compressive modulus was recorded with network degradation for up to 6 weeks. The results, shown in Figure 7, correlate relatively well to the mass-loss data. The mechanical properties of each of the polymers decreases with degradation, but happens to a greater extent depending on the polymer chemistry and structure. After 6 weeks of degradation, the compressive modulus was only ~1.5 MPa for poly(8EG6LA), but ~3.0 MPa for poly(2EG10LA). Because poly(8EG6LA) lost more

mass in this time period (~25%), a greater decrease in mechanical properties was expected because more crosslinks were cleaved throughout the network. In general, a loss of compressive modulus indicates that the network-crosslinking density is decreasing with time.

These results are indicative of a bulk-eroding mechanism with diffusion limitations. Specifically, these highly crosslinked networks may inhibit the diffusion of degradation products from the network. Diffusion limitations can affect the mass-loss profiles if all of the degradation products are not released from the polymer. Thus, the mechanics in combination with mass loss of the polymers with degradation time is very important in determining the degradation mechanism. With a surface-eroding polymer, mass loss only occurs at the surface of the sample and two things occur. First, the sample does not swell because the polymer is only eroded at the surface and not throughout the bulk of the material. Second, a surface-eroding polymer will maintain mechanics such as compressive modulus with degradation because the bulk of the material does not change. Because neither of these properties is seen, it is hypothesized that these polymers are bulk eroding even though limitations such as water permeability and diffusion of degradation products may be occurring.

During the degradation of PLA, PGA, and PLGA, the degradation timescale is highly dependent on the copolymer composition.²⁶ In general, mass loss is minimal at short timescales and accelerates as more water is able to penetrate the polymer and aid in hydrolysis. Alternatively, hydrogels formed from the polymerization of high molecular weight diacrylated PLA-PEG-PLA

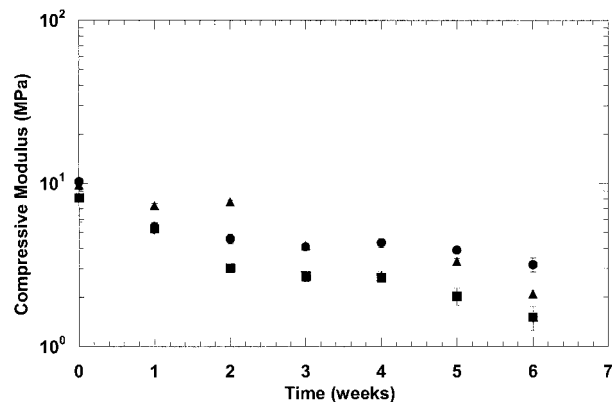


Figure 7. Compressive modulus of polymer disks with degradation in PBS at 37 °C: (▲) poly(2EG6LA); (●) poly(2EG10LA); (■) poly(8EG6LA).

macromers degrade with a distinctly different mechanism.²⁷ The high initial swelling of the gels leads to erosion rates that are much quicker than linear PLA, and the degradation products readily diffuse from the networks.²⁶ The networks formed from the low molecular weight PLA-PEG-PLA oligomers presently studied exhibit erosion profiles with characteristics of both systems. Similar to the hydrogel materials, degradation occurs through hydrolysis of the network crosslinks and results in PEG chains, lactic acid, and polyacrylate chains; however, the mass-loss profile is complicated by diffusion limitations of water into and degradation products out of the network.

Scaffold Fabrication and Characterization

For the intended application as a bone-graft-replacement material, the formation of porous polymer scaffolds in a controlled manner is important. With a bulk erosion mechanism, a scaffold is necessary for cell penetration within the polymer. Bone regeneration may then happen throughout the whole polymer scaffold rather than only at the polymer surface. Additionally, the scaffold needs to degrade in a manner that allows it to last for sufficient periods of time for cells to lay down an extracellular matrix.

Figure 8(a) shows a scaffold that was produced by polymerization in the presence of salt crystals with a range of sizes, and subsequent salt leaching. This SEM was taken from a cross section of the polymer scaffold after it was fractured. The open pore structure and lack of residual salt indicates interconnecting pores that are desirable for these polymeric scaffolds to maximize the porosity for tissue regeneration. Scaffolds with a controlled porosity were also formed using the same technique. Figure 8(b) shows a scaffold that was produced using a range of salt sizes from 150 to 300 μm . Likewise, the ratio of oligomer-to-salt particles can be altered. Note the dramatic difference in scaffold structure when a controlled distribution of salt sizes is used. The objective of these experiments was to show that scaffolds with a controlled macroscopic architecture may be readily fabricated with photopolymerization of these oligomers. Likewise, several ranges of particle sizes could be used to synergistically allow for a variety of scaffold architectures.

Scaffolds were degraded under physiological conditions. Figure 8(c) shows the cross section of a scaffold fabricated under the same conditions as Figure 8(b) that was degraded for 6 weeks. Although differences in these scaffolds are expected

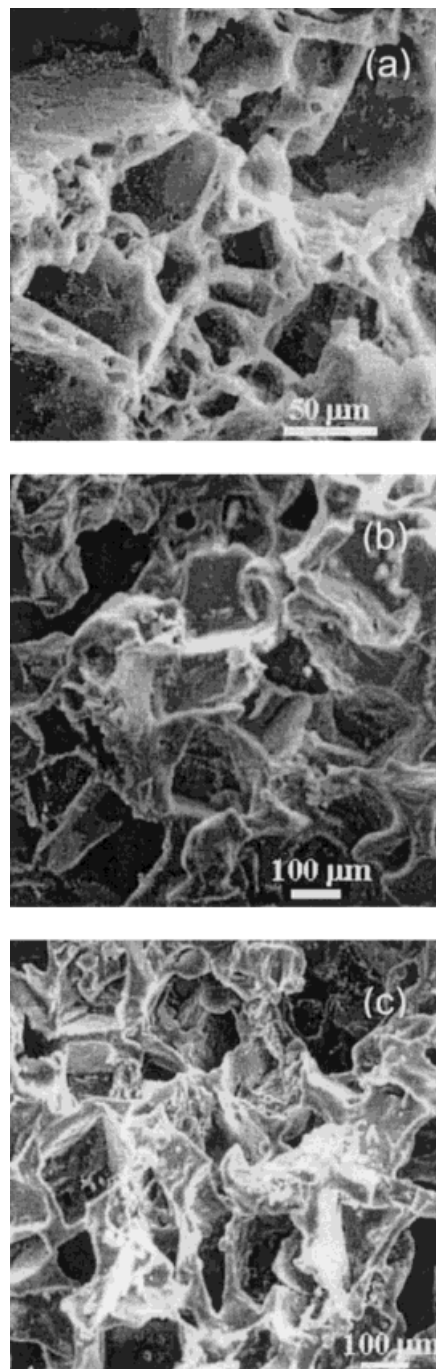


Figure 8. SEM of scaffold cross sections prepared with salt-leaching technique with 70% salt and 30 wt % 2EG10LA oligomer: (a) random-sized salt particles; (b) 150–300 μm salt particles; and (c) scaffold after 6 weeks of degradation in PBS with 150–300 μm salt particles.

based on the network chemistry and crosslinking density, the scaffold and, more importantly, a surface for cell attachment and proliferation is still remaining. The basic idea is that the scaffold

would maintain its structure long enough for bone regeneration in the pores; the scaffold degrades, and the bone-regeneration process leads to the formation of new bone to replace the previous bone defect. A recent study illustrates that PLA scaffolds prepared with the same technique degrade in a controlled fashion for significant time periods.²⁸

CONCLUSION

A class of tetrafunctional oligomers that form degradable polymer networks with potential orthopaedic applications was synthesized and characterized in the present study. These oligomers react via a controlled photoinitiated polymerization to form highly crosslinked networks within minutes using a visible-light-initiating system. Additionally, *ex vivo* implant fabrication is eliminated because these polymers may be formed *in vivo*. Both the mechanical properties and the degradation behavior of these polymers are highly dependent and controllable through alterations in the oligomer chemistry. Scaffolds with controlled macroscopic architecture that have potential to assist in bone regeneration were fabricated. Additionally, these polymers may be applicable to a wide variety of biological applications.

The authors would like to acknowledge funding from the National Science Foundation (BES-9734236), a fellowship from the Colorado Institute for Research in Biotechnology for JAB, and funding from the National Science Foundation Research Experience for Undergraduates Program in Membrane and Thin Film Science for LMP.

REFERENCES AND NOTES

- Ishaug-Riley, S. L.; Crane-Kruger, G. M.; Yaszemski, M. J.; Mikos, A. G. *Biomaterials* 1998, 19, 1405–1412.
- Boyan, B. D.; Lohmann, C. H.; Somers, A.; Niederauer, G. G.; Wozney, J. M.; Dean, D. D.; Carnes, D. L.; Schwarz, Z. J. *J Biomed Mater Res* 1999, 46, 51–59.
- Anseth, K. S.; Shastri, V. R.; Langer, R. *Nat Biotechnol* 1999, 17, 156–159.
- Griffith, L. G. *Acta Mater* 2000, 48, 263–277.
- Behraves, E.; Yasko, A.W.; Engel, P. S.; Mikos, A. G. *Clin Ortho Rel Res* 1999, 367S, S118–S125.
- Bauer, T. W.; Muschler, G. F. *Clin Orthop* 2000, 371, 10–27.
- Bos, G. D.; Goldberg, V. M.; Zika, J. M.; Heiple, K. G.; Powell, A. E. *J Bone Joint Surg Am* 1983, 65, 239–246.
- Horowitz, M.; Friedlaender, G. *Orthop Clin N Am* 1987, 18, 227–233.
- Ishaug, S. L.; Yaszemski, M. J.; Bizios, R.; Mikos, A. G. *J Biomed Mater Res* 1994, 28, 1445–1453.
- Ishaug, S. L.; Payne, R. G.; Yaszemski, M. J.; Aufdemorte, T. B.; Bizios, R.; Mikos, A. G. *Biotechnol and Bioeng* 1996, 50, 443–451.
- Muggli, D. S.; Burkoth, A. K.; Keyser, S. A.; Lee, H. R.; Anseth, K. S. *Macromolecules* 1998, 31, 4120–4125.
- Svaldi-Muggli, D.; Burkoth, A. K.; Anseth, K. S. *J Biomed Mater Res* 1998, 36, 271–278.
- Sawhney, A. S.; Pathak, C. P.; Hubbell, J. A. *Macromolecules* 1993, 26, 581–587.
- Sawhney, A. S.; Pathak, C. P.; Vanresburk, J. J.; Dunn, R. C.; Hubbell, J. A. *J Biomed Mater Res* 1994, 28, 831–838.
- Han, D. K.; Hubbell, J. A. *Macromolecules* 1997, 30, 6077–6083.
- Kim, B. S.; Hrkach, J. S.; Langer, R. *Biomaterials* 2000, 21, 259–265.
- Bryant, S. J.; Nuttelman, C. R.; Anseth, K. S. *J Biomat Sci-Poly Ed* 2000, 11, 439–457.
- Berchtold, K. A.; Bowman, C. N. *RadTech Europe 99 Conference Proceedings*, Berlin, Germany; Vincentz Publishing: Hanover, Germany, 1999; p 767.
- Mikos, A. G.; Thorsen, A. J.; Czerwonka, L. A.; Bao, Y.; Langer, R.; Winslow, D. N.; Vacanti, J. P. *Polymer* 1994, 35, 1068–1077.
- Kloosterboer, J. G. *Adv Polym Sci* 1988, 84, 1–61.
- Miyazaki, K.; Horibe, T. J. *J Biomed Mater Res* 1988, 22, 1011–1022.
- Burdick, J. A.; Peterson, A. J.; Anseth, K. S. *Biomaterials*, in press.
- Anseth, K. S.; Kline, L. M.; Walker, T. A.; Anderson, K. J.; Bowman, C. N. *Macromolecules* 1995, 28, 2491–2499.
- Tamada, Y.; Ikada, Y. *J Colloid Interface Sci* 1993, 155, 334–339.
- Hill L.W. *J Coating Technol* 1992, 64, 29–41.
- Li, S. *J Biomed Mater Res* 1999, 48, 342–353.
- Metters, A. T.; Anseth, K. S.; Bowman, C. N. *Polymer* 2000, 41, 3993–4004.
- Lu, L.; Peter, S. J.; Lyman, M. D.; Lai, H.; Leite, S. M.; Tamada, J. A.; Vacanti, J. P.; Langer, R.; Mikos, A. G. *Biomaterials* 2000, 21, 1595–1605.